Physics Letters B 690 (2010) 369–375

Contents lists available at ScienceDirect

Physics Letters B

www.elsevier.com/locate/physletb

D mesic nuclei

C. García-Recio [a,*], J. Nieves [b], L. Tolos [c]

[a] Departamento de Física Atómica Molecular y Nuclear, Universidad de Granada, 18071 Granada, Spain
[b] Departamento de Física Teórica and IFIC, Centro Mixto Universidad de Valencia–CSIC, Institutos de Investigación de Paterna, Apdo. correos 22085, 46071 Valencia, Spain
[c] Theory Group, KVI, University of Groningen, Zernikelaan 25, 9747AA Groningen, The Netherlands

ARTICLE INFO

Article history:
Received 15 April 2010
Received in revised form 19 May 2010
Accepted 20 May 2010
Available online 27 May 2010
Editor: W. Haxton

Keywords:
Charm
Mesic nuclei
Heavy quark symmetry

ABSTRACT

The energies and widths of several D^0 meson bound states for different nuclei are obtained using a D-meson selfenergy in the nuclear medium, which is evaluated in a selfconsistent manner using techniques of unitarized coupled-channel theory. The kernel of the meson–baryon interaction is based on a model that treats heavy pseudoscalar and heavy vector mesons on equal footing, as required by heavy quark symmetry. We find D^0 bound states in all studied nuclei, from ^{12}C up to ^{208}Pb. The inclusion of vector mesons is the keystone for obtaining an attractive D–nucleus interaction that leads to the existence of D^0–nucleus bound states, as compared to previous studies based on SU(4) flavor symmetry. In some cases, the half widths are smaller than the separation of the levels, what makes possible their experimental observation by means of a nuclear reaction. This can be of particular interest for the future PANDA@FAIR physics program. We also find a D^+ bound state in ^{12}C, but it is too broad and will have a significant overlap with the energies of the continuum.

1. Introduction

The D-meson–nucleus optical potential has been a subject of intense study over the last years. In particular, modifications of the D meson properties in an hadronic environment might influence the rhythm of charmonium production [1–7], as a complementary explanation for charmonium suppression in a Quark–Gluon Plasma [8]. Moreover, D-meson bound states in ^{208}Pb were predicted [9] relying upon a strong mass shift for D mesons in the nuclear medium based on a quark–meson coupling model [10]. The experimental observation of these bound states might be however problematic since, even if they exist, their widths could be very large [11] as compared to the separation of the levels. In Ref. [11], the D-meson potential was obtained using techniques of self-consistent unitarized coupled-channel theory adapted to the meson–baryon interaction [12,13], which followed and extended the works using chiral Lagrangians and the Lippmann–Schwinger equation initiated in Refs. [14,15]. This work followed a scheme similar to those used in previous approaches on the spectral features of D mesons in symmetric nuclear matter [16–19]. The systematic inclusion of medium corrections to the scattering equation is crucial for the generation and modification of the $\Lambda_c(2595)$ resonance in the nuclear medium and, thus, eliminate the main source of uncertainty of earlier evaluations of the D–nucleus optical potential. In fact, this has been also done for the η-meson selfenergy in a nuclear medium in Ref. [21], using the vacuum amplitude of Ref. [22]. The η–nucleus optical potential was evaluated in a selfconsistent way, as it was done for the antikaon case in Ref. [23]. Later this optical potential was used for studying the possible η–nucleus bound states in Ref. [24], where the energy dependence of the η selfenergy around the ηN threshold was taken into account and shown to be very much relevant for the problem.

Here we will undertake a similar study for the D^0–nucleus bound states using a recently generated D meson selfenergy in the nuclear medium [25]. This model incorporates heavy-quark symmetry in the charm sector improving in this respect with the recent t-channel vector meson-exchange approaches [11,18–20]. As a consequence, the pseudoscalar D meson and the D^* meson, its vector partner, are treated on equal footing. This new scheme generates a broad spectrum of new resonant meson–baryon states in the charm one and strangeness zero [26] and the exotic charm minus one [27] sectors. Furthermore, this framework allows to obtain simultaneously the properties of D and D^* mesons in nuclear matter [25]. The in-medium calculation of Ref. [25] includes Pauli blocking effects on the nucleon and the D and D^* selfenergies in a self-consistent manner. Moreover, in this work, a novel renormalization scheme is introduced that guaranties that the nuclear medium corrections do not depend on the ultraviolet cutoff used to renormalize the free space amplitudes. Compared to previous results [11,19], the width of the D meson in nuclear matter is small with respect to the mass shift and, therefore, bound states for D mesons in nuclei might be expected.

* Corresponding author.
E-mail address: g_recio@ugr.es (C. García-Recio).

0370-2693
doi:10.1016/j.physletb.2010.05.056

This Letter is organized as follows. In Section 2 we introduce the D–nucleus potential from Ref. [25]. The results for the different D–nucleus bound states are discussed in Section 3, where we also compare with other microscopical models. The conclusions are drawn in Section 4.

2. The D–nucleus optical potential

In Ref. [25] the selfenergy of the D meson is evaluated in nuclear matter at various densities, ρ, as a function of the D energy, q^0, and its momentum, $\vec{q}$, in the nuclear matter frame. It is calculated by means of

$$\Pi_D(q^0,\vec{q},\rho) = \int_{p\leqslant p_F} \frac{d^3p}{(2\pi)^3}\big[T_{DN}^{\rho\,(I=0,J=1/2)}(P^0,\vec{P}) + 3T_{DN}^{\rho\,(I=1,J=1/2)}(P^0,\vec{P})\big], \tag{1}$$

where $\vec{p}$ and p_F are the momentum of the nucleon and the Fermi momentum at nuclear density ρ, respectively. The quantity $T_{DN}^{\rho}(P^0,\vec{P})$ is the in-medium DN s-wave interaction, with total four-momentum $(P^0,\vec{P})$ in the nuclear matter frame, namely $P^0 = q^0 + E_N(\vec{p})$ and $\vec{P} = \vec{q} + \vec{p}$. Here, isospin symmetry is assumed, and the amplitude is summed over nucleons up to the Fermi level. Since we are interested in finding bound states, we shall be concerned about the s-wave D selfenergy around the DN threshold.

The in-medium interaction T_{DN}^{ρ} is obtained self-consistently including all coupled channels with the same quantum numbers. In the work of Ref. [25], the Bethe–Salpeter equation is solved with sixteen coupled channels for $I=0$, $J=1/2$, twenty-two channels for $I=1$, $J=1/2$, eleven channels for $I=0$, $J=3/2$ and twenty for $I=1$, $J=3/2$. The medium effects in the scattering amplitude are the Pauli blocking on the intermediate nucleon states and the selfenergy of the charmed mesons (D and D^*) in the intermediate channels. The pion and baryon selfenergies are not considered. While the baryon dressing did not change the qualitative behaviour of the D meson in nuclear matter [11], the coupling to intermediate states with pions is of minor importance for the DN and D^*N dynamics in a dense environment [25]. Note the importance of the selfconsistency for $\Pi_D(q^0,\vec{q};\rho)$, since the in-medium amplitude T_{DN}^{ρ} contains the $D(D^*)N$ channel, which depends in turn on $\Pi_{D(D^*)}(q^0,\vec{q};\rho)$.

The D selfenergy, scaled by $2m_D$, is displayed with points in Fig. 1 as a function of the D-meson energy around threshold. It is shown for various nuclear medium densities, ρ, and with the D meson momentum fixed to zero.

The D selfenergy is evaluated in infinite nuclear matter. In finite nuclei we use the local density approximation (LDA), substituting ρ by $\rho(r)$, which is the local density at each point in the nucleus taken from experiment. For the s-wave, as it is here the case, it was shown in Ref. [28] that LDA gave the same results as a direct finite nucleus calculation. Then, the LDA D selfenergy, $\Pi_D(q^0,r) \equiv \Pi_D(q^0,\vec{0},\rho(r))$ allows to define an energy-independent local optical potential,

$$V_D(r) = \frac{\Pi_D(q^0 = m_D,\vec{q}=0,\rho(r))}{2m_D}, \tag{2}$$

from its threshold ($q^0 = m_D$, $\vec{q}=0$) value. This prescription gives a potential of $(-25-i14)$ MeV at normal nuclear matter density $\rho_0 = 0.17$ fm^{-3} as can be read off from Fig. 1. This would mean that one can expect bound states with approximately -20 MeV binding and a half-width of about 14 MeV.

However, both the real and the imaginary parts of the D selfenergy, around the D-meson mass, show a pronounced energy dependence, as can be appreciated in Fig. 1. For instance, the real part at $q^0 - m_D = -20$ MeV is about one forth of its value at $q^0 = m_D$. Hence, a realistic determination of the D bound states should take this energy dependence into account. Thus, we use an energy-dependent optical potential defined as:

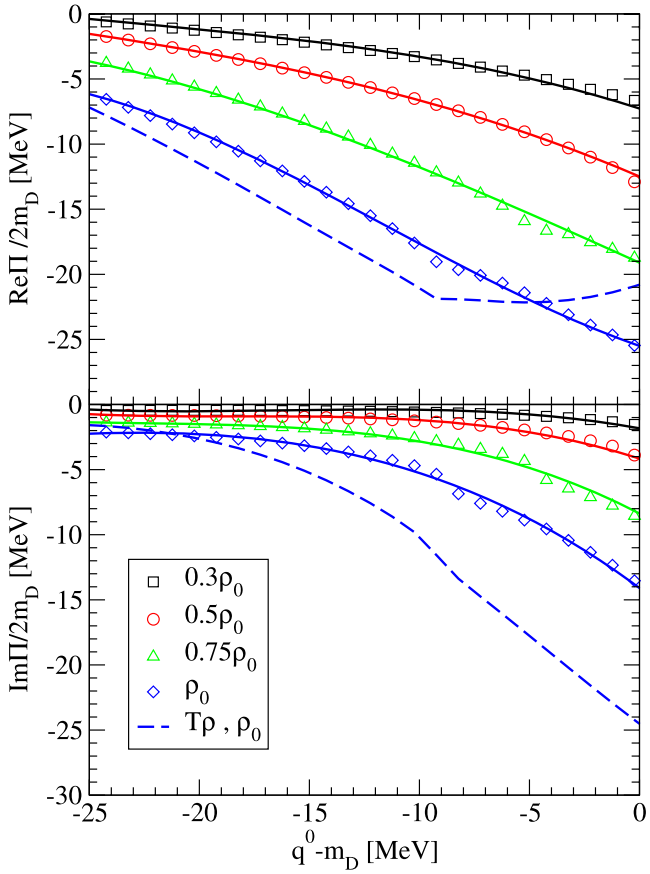

Fig. 1. Selfconsistent D selfenergy of Ref. [25] for zero momentum as a function of energy, and for four different densities. The solid lines stand for the fitted functions of Eqs. (4)–(5). The dashed line shows the selfenergy for $\rho = \rho_0$ calculated in the low density limit (without selfconsistency).

$$V_D(r,E) = \frac{\Pi_D(q^0 = m_D + E,\vec{q}=0,\rho(r))}{2m_D}, \tag{3}$$

where $E = q^0 - m_D$ is the D^0 energy excluding its mass. In order to use the potential defined above in Eq. (3), the results of Ref. [25] are parameterized in terms of analytical functions in the energy range -25 MeV $< E < 0$ as (see the solid lines in Fig. 1),

$$\begin{aligned}&\mathrm{Re}\big[\Pi_D\big(q^0 = m_D + E,\vec{0},\rho\big)\big] = a(\rho) + b(\rho)E + c(\rho)E^2 + d(\rho)E^3,\\ &\mathrm{Im}\big[\Pi_D\big(q^0 = m_D + E,\vec{0},\rho\big)\big]\\ &\quad = e(\rho) + f(\rho)E + g(\rho)E^2 + h(\rho)E^3,\end{aligned} \tag{4}$$

with

$$\begin{aligned}a(\rho) &= \big(-84033.1\rho/\rho_0 - 25727.8\rho^2/\rho_0^2\\ &\qquad + 14536.2\rho^3/\rho_0^3\big)\ \mathrm{MeV}^2,\\ b(\rho) &= \big(-8654.6\rho/\rho_0 + 6475.6\rho^2/\rho_0^2\big)\ \mathrm{MeV},\\ c(\rho) &= -341.2\rho/\rho_0 + 447.8\rho^2/\rho_0^2,\\ d(\rho) &= \big(-5.648\rho/\rho_0 + 8.777\rho^2/\rho_0^2\big)\ \mathrm{MeV}^{-1},\end{aligned}$$

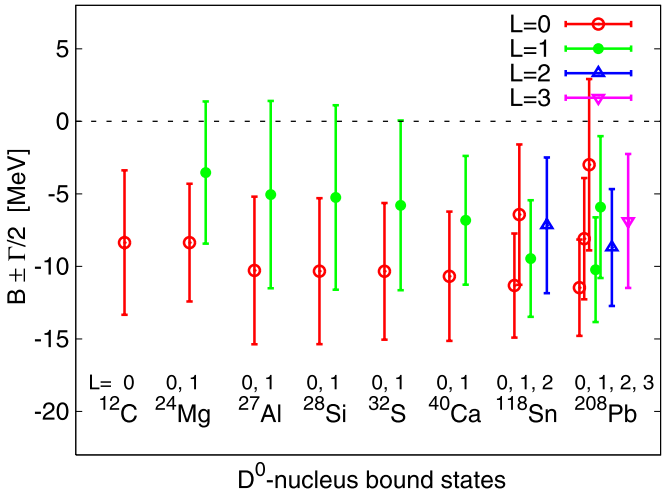

Fig. 2. Binding energies and widths for different D^0–nucleus states obtained using the strong energy-dependent D-potential.

$$
\begin{aligned}
e(\rho) &= \left(-10616.5\rho/\rho_0 - 39532.6\rho^2/\rho_0^2 \right.\\
&\quad \left. - 2489.6\rho^3/\rho_0^3\right)\ \text{MeV}^2,\\
f(\rho) &= \left(-3356.6\rho/\rho_0 - 1337.44\rho^2/\rho_0^2\right)\ \text{MeV},\\
g(\rho) &= -291.09\rho/\rho_0 + 136.656\rho^2/\rho_0^2,\\
h(\rho) &= \left(-6.70\rho/\rho_0 + 5.20\rho^2/\rho_0^2\right)\ \text{MeV}^{-1}.
\end{aligned}
\tag{5}
$$

In the next section we will solve the Schrödinger equation, with both the energy-dependent [Eq. (3)] and independent [Eq. (2)] potentials, to find bound states for different nuclei through the periodic table. Since the D-meson optical potential is much smaller than its mass, we expect the relativistic corrections to be tiny and certainly smaller than the theoretical uncertainties of the interaction. We will also discuss the implications of our results in the practical search for these D^0 bound states.

3. Results

We look for D^0–nucleus bound states by solving the Schrödinger equation:

$$
\left[-\frac{\vec{\nabla}^2}{2\mu} + V_{\text{opt}}(r)\right]\Psi = (B - i\Gamma/2)\Psi, \tag{6}
$$

where B is the binding energy ($B < 0$), $\Gamma/2$ the half-width of the bound state and μ is the D–nucleus reduced mass. As mentioned above, we will present results from two different potentials $V_{\text{opt}}(r) = V_D(r, E = B)$ and $V_{\text{opt}}(r) = V_D(r, E = 0)$.

We solve the Schrödinger equation in coordinate space by using a numerical algorithm [29,30], which has been extensively tested in similar problems of pionic [28,31] and antikaonic [32] atomic states and in the search of possible antikaon–nucleus [32] and η–nucleus [24] bound states. Charge densities are taken from Ref. [33]. For each nucleus, we take the neutron matter density approximately equal to the charge one, though we consider small changes, inspired by Hartree–Fock calculations with the DME (density-matrix expansion) [34] and corroborated by pionic atom analysis [35]. In Table 1 of Ref. [32] all the densities used throughout this work can be found. However, charge (neutron matter) densities do not correspond to proton (neutron) ones because of the finite size of the proton (neutron). We take that into account following the lines of Ref. [28] and use the proton (neutron) densities in our approach.

Results, binding energies and widths, from the energy-dependent potential are shown in Table 1. These results are also presented in Fig. 2, where the states found for different nuclei and orbital angular momentum are collected. The bound states for which the absolute value of the binding energy is much smaller than the corresponding half width have not been presented, because they mix with the continuum energy spectrum and do not define clear bound states. For instance, in ^{40}Ca we also find a $2s$ state with a binding energy of -1.3 MeV and half-width of 6.7 MeV, which mixes with the continuum. We have disregarded the consideration of this state and others alike.

From the results of Table 1, we conclude there exist chances to see distinct peaks corresponding to D^0 bound states. Let us consider angular momentum $l = 0$. For medium size nuclei, up to ^{40}Ca, there exists only one relevant D^0 bound state in each nucleus, with a binding energy around -10 MeV and half-width roughly below 5 MeV, which can be subject to experimental detection. For heavier nuclei, like ^{118}Sn and ^{208}Pb, we find two $l = 0$ bound states, with an energy separation similar to their half-widths (around 4 MeV). In the case of angular momentum $l = 1$, and for medium size nuclei (from ^{24}Mg up to ^{32}S) we find only the $1p$ state, with $|B|$ smaller or equal than the $\Gamma/2$. Thus, these states are in the edge of the possible experimental determination. For heavier nuclei like ^{40}Ca and ^{118}Sn there is a well defined $1p$ bound state. In the case of ^{208}Pb, we find the $1p$ and $2p$ bound states separated by 4.3 MeV, while their half-widths are 3.6 and 4.9 MeV, respectively. We also find states with $l = 2$ for ^{118}Sn and ^{208}Pb, and $l = 3$ for ^{208}Pb.

In summary, for light and medium nuclei (from $A = 12$ up to $A = 40$), there are observable D^0 mesic nuclei $1s$ states. For heavier nuclei, and in addition to the $1s$ level, we also find clearly observable $1p$ states assuming that different angular momentum can be separated. For all cases, the bound D^0 meson is not orbiting around the nucleus, but rather it is embedded inside of it. For instance this can be seen in the left panel of Fig. 3, where the squared absolute values of the radial wave function for the $1s$ and $1p$ levels in ^{208}Pb, together with the nuclear density, are shown.

To clarify the most relevant aspects of the model, we have also obtained the bound state spectrum when some of the ingredients of the full model are not considered. In Table 2, we show results for ^{12}C, ^{40}Ca and ^{208}Pb nuclei with different approximations. First, we examine the effects produced by the strong energy dependence of the optical potential and have computed energies and widths with the energy-independent optical potential of Eq. (2). We see that when the energy dependence of the potential is neglected, the states become more bound by a factor ranging from 1.6 in ^{12}C to 2 in ^{208}Pb, and also the widths of the states became larger by approximately a factor of two. These results can be easily understood by looking at the energy dependence of the optical potential in Fig. 1. There, we see that both, the real (attractive) and imaginary (negative) parts of the optical potential decrease, in absolute value, by a factor larger than 2 from the threshold, $q^0 = m_D$, to $q^0 = m_D - 15$ MeV. Thus, the energy dependence of the optical potential plays a major role and need to be taken into account.

Next, we examine in Table 2 the importance of the selfconsistency in the calculation. To this end, we have recalculated the full spectrum by using an energy-dependent optical potential deduced from the D selfenergy in the low density limit, $\Pi_{\text{low}} \sim T\rho$, where T is the ND T-matrix in free space. This amounts to use $T^{\rho=0}$, instead of T^{ρ} in Eq (1). In Fig. 1, we also compare the D selfenergy calculated for normal nuclear matter density with and without selfconsistency for zero momentum and energies below threshold. Though, the real part of the $\Pi_D(q^0, \vec{0}, \rho)$ selfconsistent selfenergy does not differ much from that of the low density theorem approach, however, the absolute values of the imaginary

Table 1
$(-B,\ \Gamma/2)$ in MeV for D^0–nucleus bound states calculated with the energy-dependent selfenergy.

	^{12}C	^{24}Mg	^{27}Al	^{28}Si	^{32}S	^{40}Ca	^{118}Sn	^{208}Pb
1s	(7.0, 5.0)	(8.4, 4.1)	(10.3, 5.1)	(10.3, 5.0)	(10.3, 4.7)	(10.7, 4.5)	(11.3, 3.6)	(11.5, 3.3)
1p		(3.5, 4.9)	(5.0, 6.5)	(5.3, 6.4)	(5.8, 5.9)	(6.8, 5.4)	(9.5, 4.0)	(10.2, 3.6)
1d							(7.2, 4.7)	(8.7, 4.0)
2s							(6.4, 4.8)	(8.1, 4.2)
1f								(6.9, 4.6)
2p								(5.9, 4.9)

Table 2
$(-B,\ \Gamma/2)$ in MeV for D^0–nucleus bound states in ^{12}C, ^{40}Ca and ^{208}Pb. The first set of results have been obtained by using the energy-independent potential of Eq. (2). In the second set of results, though the energy dependence of the optical potential is kept, binding energies and widths have been obtained from a low density optical potential, where effects due to the selfconsistency treatment have been neglected. The last column gives, for comparison, the predicted binding energies of Ref. [9] for ^{208}Pb (in MeV).

	Energy-independent $V_{\rm opt}$			Energy-dependent $V_{\rm opt}$ without selfconsistency			$-B$ of Ref. [9]
	^{12}C	^{40}Ca	^{208}Pb	^{12}C	^{40}Ca	^{208}Pb	^{208}Pb
1s	(11.1, 10.9)	(18.4, 13.5)	(20.2, 11.0)	(7.5, 10.2)	(12.2, 7.5)	(13.0, 5.2)	96.2
1p		(11.0, 11.4)	(17.9, 10.7)		(7.3, 11.1)	(6.6, 9.5)	93.0
1d			(15.0,10.3)			(2.6, 12.8)	
2s			(13.9,10.1)			(1.5, 13.7)	88.5
1f			(11.7,9.8)				
2p			(9.9,9.5)				

part of the $\Pi_{\rm low}$ approach are around a 60% larger than the exact result of $\Pi_D(q^0, \vec{q}=0, \rho)$ for $\rho=\rho_0$, and in the energy region -20 MeV $\leqslant q^0 - m_D \leqslant 0$. As a consequence, the obtained bound states (see Table 2) using the low density limit have larger widths and smaller binding energies (due to the repulsive effect of the larger imaginary part) than those calculated with the exact self-consistent potential.

After analyzing the relevance of the ingredients of the model, we also compare our results in ^{208}Pb with those obtained in Ref. [9]. There, a relativistic mean field calculation is carried out that leads to binding energies much larger than those obtained here. For instance, the 1s state in ^{208}Pb is bound by almost one hundred MeV and has no width in the model of Ref. [9], whereas we find a binding of only about ten MeV with a width of 6.6 MeV for the same 1s level (see Table 2). Of course, our coupled channel unitary and selfconsistent model is much more elaborated and it is also able to predict decay widths.

Finally, we address the possibility of finding D^+ mesic nuclei. The calculated D–nucleus strong optical potential is the same for D^0 and D^+ mesons because of the isospin symmetry. The found full optical potential is not very deep. The strength of the attractive potential is, at most, 20 MeV (see Fig. 1). A positive charged D^+ meson also feels the nuclear attraction of the nuclei. However, the Coulomb repulsion due to the positive electric charge of the nuclei is important, especially for heavy nuclei. We have considered a light nuclei, ^{12}C, and studied the D^+–nucleus bound states by adding the Coulomb repulsive potential to the optical one. We have found that the 1s state has a binding energy of $B=-4.6$ MeV and a half-width of $\Gamma/2=6.4$ MeV which is larger that $|B|$. Hence this state is not a clear case for experiments because it has a significant overlap with the energies of the continuous energy spectrum. Obviously for heavier nuclei, with more protons, there is not a better chance of finding D^+–nucleus bound states. We do not study the case of nuclei lighter than ^{12}C, because the LDA used here is not reliable enough for small nuclei, specially when significant cancellations among Coulomb and optical potential are taking place. Summarizing, with the optical potential considered in this work, there are no chances of finding D^+ mesic nuclei with atomic number Z equal or larger than 6.

In the coupled channel calculation of Ref. [25], used as input for the D meson optical potential of this work, the nuclear matter vector meson D^* selfenergy was calculated as well. The in-medium D^* selfenergy is found there to be repulsive for energies around the threshold and densities $\rho \leqslant \rho_0$, hence that model predicts that there are not D^*–nucleus bound states.

The SU(8) model used here as a kernel in the coupled channel unitary calculation reduces to the SU(4) model for $J=1/2$, when the vector meson coupling constants are set to zero. To establish the relevance of the inclusion of the vector mesons, specially of the D^*, in the D meson dynamics, we have also performed the calculations with the SU(4) model. In the left panel of Fig. 4, both the SU(8) and SU(4) D selfenergies are displayed for comparison. There, it can be appreciated that at threshold ($q^0=m_D$) and for $\rho \leqslant \rho_0$, the SU(4) potential is small and repulsive, while the SU(8) model provides a small attraction. However, for $q^0 - m_D = -15$ MeV and $\rho \leqslant \rho_0$, both potentials are attractive. However, the imaginary parts of both selfenergies are quite different, being much larger for the SU(4) case (about -60 MeV for $\rho=\rho_0$) than for the SU(8) model. This is due to the behaviour at finite density of the different resonance–hole structures of the D-meson selfenergy close to the DN threshold in the SU(4) [11,19] and SU(8) [25] models. The large imaginary part of the SU(4) optical potential induces an effective repulsion, which together with the small attraction of its real part leads to the no existence of D^0–nucleus bound states within the SU(4) model. This is in contrast to the SU(8) model that turns out to be attractive enough to give the bound spectra shown in Table 1 and Fig. 2.

A word of caution must be said here. The above discussion overlooks the fact there will be some extra contributions to the D-selfenergy from the $DN \to D^*N$ interaction mediated by pion exchange from the p-wave $D^* \to D\pi$ and $NN\pi$ vertices (see right panel of Fig. 4). At threshold, these extra terms will be purely real, since there is no phase space for the reaction $DN \to D^*N$, and they would also affect to the s-wave free space amplitudes derived in Ref. [26]. Because of the p-wave nature of the involved vertices, we expect the s-wave part of these contributions to be small near threshold, and their contribution to be effectively accounted for by the renormalization parameters used in [26], that were adjusted to reproduced the lowest-lying s-wave charmed baryon resonances. Note, however, that these new mechanisms will be source of extra imaginary part in the case of the D^*-selfenergy.

4. Conclusions

We have used a recent D^0–nucleus optical potential, evaluated within a self-consistent unitarized coupled-channel approach to

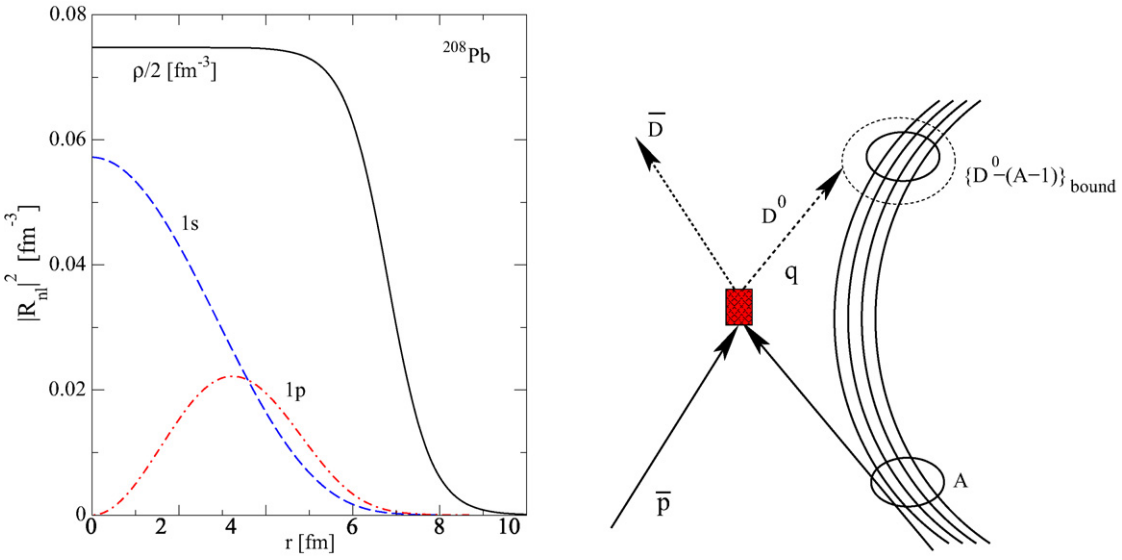

Fig. 3. Left: Squared absolute value of the radial part of the wave function of the $1s$ and $1p$ levels in ^{208}Pb. The nuclear density for ^{208}Pb is also shown. Right: Possible mechanism for production of D^0 mesic nuclei using a beam of antiprotons.

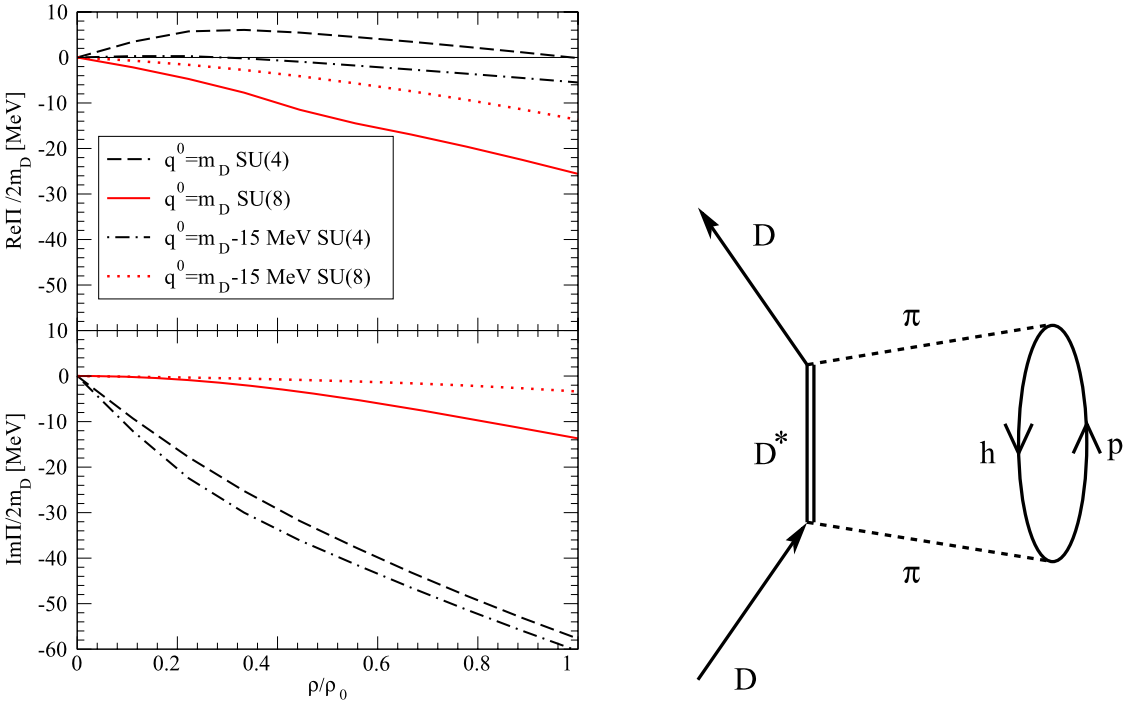

Fig. 4. Left: Comparison of the Π_D selfenergy over $2m_D$ versus nuclear density for different values of the meson energy $q^0 = m_D$ and $q^0 = m_D - 15$ MeV for SU(8) and SU(4) models. Right: Contribution to the D-selfenergy induced by the p-wave $D^* \to D\pi$ and $NN\pi$ vertices.

find D^0–nucleus bound states. We have shown that selfconsistency effects and the energy dependence of the optical potential play major roles, and need certainly to be taken into account. The potential is attractive and we find bound states for all studied nuclei through the whole periodic table. On the other hand, it produces states with relatively small half widths, smaller in general than the binding energies, and in many cases smaller than the separation among levels, which makes possible their observation.

The strong energy dependence of the potential is due to the large effect on the D selfenergy of the charmed resonances, and their medium modifications [25], appearing close to DN threshold [26]. Taking into account the energy dependence reduces the strength of both the real and imaginary parts of the potential, below the D^0 threshold. This leads to substantially narrower states, but at the same time also with smaller binding energies. The heavy nuclei accommodate many D^0-bound states and the separation of the levels, for a fixed angular momentum, is about half width of the states. The best chances for observation of bound states are in the region of ^{24}Mg, provided an orbital angular momentum separation can be done, where there is only one s-bound state and its half width is about a factor of two smaller than the binding energy. In any case we would like to stress out that even if no broad bumps are found in the experiments, they should find some strength in the bound region stretching in energy down to the

sum of the binding energy plus the half width of the bound states. Short of having the values for the binding energy and width of the states, this more limited information is still very valuable to gain some knowledge on the D–nucleus optical potential, and it should stimulate experiments in this direction. This can be of particular interest for the future PANDA@FAIR physics program. Nevertheless, we should point out that the production and the experimental detection of these D^0–nucleus bound states will likely be a quite difficult task. One might think in reactions of the type (see right panel of Fig. 3)

$$\begin{aligned}\bar{p} + A_Z &\to D^- + \left\{(A-1)_Z - D^0\right\}_{\text{bound}} \\ &\to \bar{D}^0 + \left\{(A-1)_{Z-1} - D^0\right\}_{\text{bound}} \end{aligned} \tag{7}$$

to be investigated in the future facility FAIR. Since the above reactions are two-body → two-body, the outgoing $\bar{D}$ energy is fixed, for a certain scattering angle in the laboratory system, and the creation of the D^0 bound state will be identified as a peak in the $d\sigma/d\Omega\, dE(\bar{D})$ over a background of inclusive $(\bar{p}, \bar{D})$ cross section. The High-Energy Storage Ring (HESR) at FAIR running with full luminosity (limited by the production rate of $2 \times 10^7\, \bar{p}/s$) at momenta larger than 6.4 GeV would produce about 100/s D meson pairs around $\psi(4040)$ [36]. Assuming that one per ten million[1] of the produced D^0 mesons is trapped in a bound orbit, we are then left with a production rhythm of around only one event every 10^5 seconds or equivalently to few hundred events per year.

Recoilless production reactions have proved to be more efficient in the case of detecting deeply pionic bound states [38–40]. One possible reaction, where negligible momentum transfers could be achieved, is

$$D^{*+} + A_Z \to \pi^+ + \left\{A_Z - D^0\right\}_{\text{bound}}. \tag{8}$$

From the theoretical point of view we would expect sizeable formation peaks over a flat background. However, since the D^* is an unstable particle, it will not be possible to create a D^* beam, which makes, in practice, unfeasible the above reaction.[2] The above discussion brings us to reconsider the reactions of Eq. (7), and creating in the primary $\bar{p}N$ collision, not only a $D\bar{D}$ pair, but also a virtual pion, which will induce many body modes (particle–hole) in the nuclear medium [42]. Such modes will carry almost no energy, but high momentum components, which would allow the virtual D^0 meson in the right panel of Fig. 3 to have a significantly smaller momentum, being in this way, significantly increased the D^0 bound state production cross section. The main drawback would be that one is not facing now with a two-body going to two-body reaction. Hence to guaranty the creation of the D^0–nucleus bound state, it would be needed to look at the decay products, $\Lambda_c\pi$ and $\Sigma_c\pi$ pairs, after the absorption of the D^0 by the nucleus. However, once the decay products of D^0–nucleus bound state need to be detected, one realizes that it is unnecessary to use antiprotons (secondary beam) as projectiles, and instead one can benefit from the use of protons (primary beam), obtaining in this way a large enhancement factor ($\sim 10^5$) in the incoming flux. Thus, one could look at reactions of the type

$$p + A_Z \to p + \bar{D}^0 + \underbrace{\left\{A_Z - D^0\right\}_{\text{bound}}}_{\hookrightarrow\ \Lambda_c\pi + X,\ \Sigma_c\pi + X}. \tag{9}$$

Given the fact that there are more that two particles in the final state, it is possible to pick up regions of the phase space where the momentum, that needs to be accommodated in the D^0 bound wave function, would be sufficiently small to make significantly larger the probability of D^0 trapping. Moreover, the above reaction is coherent; there is no change of charge in $p + N \to p + \bar{D}^0 + D^0 + N$ and the final nuclear state is the same as the initial one. This provides a factor A^2 in the cross section versus a factor A in the inclusive reaction which gives the background [38]. Because of that, D^0-bound states in heavier nuclei than magnesium, mentioned above, might have better chances to be detected.

Finally, we would like to point out that in this work we have used a model for the in medium D-meson selfenergy that, it is based on a SU(8) spin–flavor extension [26] of the SU(2) Weinberg–Tomozawa (WT) pion–nucleon s-wave interaction in the free space.[3] When vector mesons are not considered, our in medium selfenergy reduces, up to minor details, to that deduced in Ref. [19]. This latter one is based on a SU(4) flavor extension of the SU(2) vacuum WT pion–nucleon s-wave interaction. The optical potential deduced from Ref. [19] is not attractive enough to bind D^0 nuclear states. This is in sharp contrast with our findings here. One of the major differences between both approaches, and mostly responsible for this distinctive difference, is that the model used here treats heavy pseudoscalar and heavy vector mesons on equal footing, as required by Heavy Quark Symmetry (HQS). This latter symmetry is a proper QCD spin–flavor symmetry [43–45] when the quark masses become much larger than the typical confinement scale, Λ_{QCD}.

Acknowledgements

We warmly thank B.S. Zou, A. Gillitzer and E. Oset for useful discussions. This work is partly supported by DGI and FEDER funds, under contract FIS2008-01143/FIS, the Spanish Ingenio-Consolider 2010 Program CPAN (CSD2007-00042), the Junta de Andalucia grant No. FQM225, and Generalitat Valenciana under contract PROMETEO/2009/0090. We acknowledge the support of the European Community Research Infrastructure Integrating Activity "Study of Strongly Interacting Matter" (acronym HadronPhysics2, Grant Agreement No. 227431) under the Seventh Framework Programme of EU. Work supported in part by DFG (SFB/TR 16, "Subnuclear Structure of Matter"). L.T. acknowledges support from the RFF program of the University of Groningen and the Helmholtz International Center for FAIR within the framework of the LOEWE program by the State of Hesse (Germany).

[1] This fraction should be understood only as an educated guess. In reactions of the type of that of Fig. 3, the momentum transferred q to the bound D^0 is fixed. The cross section for the reaction is then proportional to $|\Phi_{nlm}(q)|^2$, where $\Phi_{nlm}(q)$ is the D^0 bound wave function in momentum space [37,38]. Since in the reactions of Eq. (7) the momentum transfer is quite large, around 2 GeV at threshold, and at least 1 GeV for incoming antiproton momenta of 10 GeV or larger, one can immediately see that the cross sections will be small, since the D^0 bound wave function has difficulty to accommodate such large momenta; but the reaction is possible. Given the typical size of the D^0 bound states (see for instance the left panel of Fig. 3), momentum transfers of about 0.2 GeV can be easily accommodated, and in these circumstances one might expect that one per cent of the D^0 mesons could be trapped [37,38]. The extra six orders of magnitude of reduction, implicit in the fraction 10^{-7}, would account for the expected large reduction of the D^0 bound wave function when the momentum increases from 0.2 GeV to 1 GeV (we have assumed a factor 10^{-3}).

[2] Around ten millions of $\bar{D}^{(*)}D^{(*)}$ pairs per year are expected to be produced at BESIII in the region of the $\psi(3770)$ and $X(4160)$ resonances [41]. Even if it were possible to put a thin nuclear target of 1 cm^2 at a distance at small as 1 meter from the collision area, we would not have more than one per year charmed meson interacting with the nuclear target.

[3] Of course, both flavor and spin symmetry breaking terms are included in the model of Ref. [26] to account for the physical hadron masses and meson decay constants.

References

[1] W. Cassing, E.L. Bratkovskaya, Phys. Rep. 308 (1999) 65.
[2] R. Vogt, Phys. Rep. 310 (1999) 197.
[3] C. Gerschel, J. Hüfner, Annu. Rev. Nucl. Part. Sci. 49 (1999) 255.
[4] X.N. Wang, B. Jacak (Eds.), Quarkonium Production in High-Energy Nuclear Collisions, World Scientific, 1998.
[5] A. Capella, E.G. Ferreiro, A.B. Kaidalov, Phys. Rev. Lett. 85 (2000) 2080.
[6] A. Andronic, P. Braun-Munzinger, K. Redlich, J. Stachel, Phys. Lett. B 659 (2008) 149.
[7] O. Linnyk, E.L. Bratkovskaya, W. Cassing, Int. J. Mod. Phys. E 17 (2008) 1367.
[8] T. Matsui, H. Satz, Phys. Lett. B 178 (1986) 416.
[9] K. Tsushima, D.H. Lu, A.W. Thomas, K. Saito, R.H. Landau, Phys. Rev. C 59 (1999) 2824.
[10] A. Sibirtsev, K. Tsushima, A.W. Thomas, Eur. Phys. J. A 6 (1999) 351.
[11] L. Tolos, A. Ramos, T. Mizutani, Phys. Rev. C 77 (2008) 015207.
[12] E. Oset, A. Ramos, Nucl. Phys. A 635 (1998) 99.
[13] J.A. Oller, U.G. Meissner, Phys. Lett. B 500 (2001) 263.
[14] N. Kaiser, P.B. Siegel, W. Weise, Nucl. Phys. A 594 (1995) 325.
[15] N. Kaiser, T. Waas, W. Weise, Nucl. Phys. A 612 (1997) 297.
[16] L. Tolos, J. Schaffner-Bielich, A. Mishra, Phys. Rev. C 70 (2004) 025203.
[17] L. Tolos, J. Schaffner-Bielich, H. Stoecker, Phys. Lett. B 635 (2006) 85.
[18] M.F.M. Lutz, C.L. Korpa, Phys. Lett. B 633 (2006) 43.
[19] T. Mizutani, A. Ramos, Phys. Rev. C 74 (2006) 065201.
[20] C.E. Jimenez-Tejero, A. Ramos, I. Vidana, Phys. Rev. C 80 (2009) 055206.
[21] T. Inoue, E. Oset, Nucl. Phys. A 710 (2002) 354.
[22] T. Inoue, E. Oset, M.J. Vicente Vacas, Phys. Rev. C 65 (2002) 035204.
[23] A. Ramos, E. Oset, Nucl. Phys. A 671 (2000) 481.
[24] C. Garcia-Recio, T. Inoue, J. Nieves, E. Oset, Phys. Lett. B 550 (2002) 47.
[25] L. Tolos, C. Garcia-Recio, J. Nieves, Phys. Rev. C 80 (2009) 065202.
[26] C. Garcia-Recio, V.K. Magas, T. Mizutani, J. Nieves, A. Ramos, L.L. Salcedo, L. Tolos, Phys. Rev. D 79 (2009) 054004.
[27] D. Gamermann, C. Garcia-Recio, J. Nieves, L.L. Salcedo, L. Tolos, Phys. Rev. D 81 (2010) 094016.
[28] J. Nieves, E. Oset, C. Garcia-Recio, Nucl. Phys. A 554 (1993) 509.
[29] E. Oset, L.L. Salcedo, J. Comput. Phys. 57 (1985) 361.
[30] C. Garcia-Recio, E. Oset, L.L. Salcedo, D. Strottman, M.J. Lopez, Nucl. Phys. A 526 (1991) 685.
[31] J. Nieves, E. Oset, C. Garcia-Recio, Nucl. Phys. A 554 (1993) 554.
[32] A. Baca, C. García-Recio, J. Nieves, Nucl. Phys. A 673 (2000) 335.
[33] C.W. de Jager, H. de Vries, C. de Vries, At. Data Nucl. Data Tables 14 (1974) 479;
C.W. de Jager, H. de Vries, C. de Vries, At. Data Nucl. Data Tables 36 (1987) 495.
[34] J.W. Negele, D. Vautherin, Phys. Rev. C 11 (1975) 1031, and references therein.
[35] C. García-Recio, J. Nieves, E. Oset, Nucl. Phys. A 547 (1992) 473.
[36] Baseline Technical Report September 2006, vol. 3B: Technical Progress Report for P̄ANDA, http://www.gsi.de/fair/reports/btr.html.
[37] J. Nieves, E. Oset, Nucl. Phys. A 518 (1990) 617.
[38] J. Nieves, E. Oset, Phys. Lett. B 282 (1992) 24.
[39] S. Hirenzaki, H. Toki, T. Yamazaki, Phys. Rev. C 44 (1991) 2472.
[40] K. Itahashi, et al., Phys. Rev. C 62 (2000) 025202.
[41] B.S. Zou, private communication.
[42] E. Hernandez, E. Oset, Z. Phys. A 341 (1992) 201.
[43] N. Isgur, M.B. Wise, Phys. Lett. B 232 (1989) 113.
[44] M. Neubert, Phys. Rep. 245 (1994) 259.
[45] A.V. Manohar, M.B. Wise, Heavy Quark Physics, Cambridge Monographs on Particle Physics, Nuclear Physics and Cosmology, vol. 10, Cambridge Univ. Press, 2000.